The multi-time-scale correlations for drought–flood index to runoff and North Atlantic Oscillation in the headstreams of Tarim River, Xinjiang, China

Hongbo Ling, Xiaoya Deng, Aihua Long and Haifeng Gao

ABSTRACT

The multi-time-scale correlations for the drought–flood index to annual runoff and North Atlantic Oscillation (NAO) in the past 50 years were analyzed by collecting monthly precipitation and annual runoff data and employing the methods of the *Z* index and wavelet analysis in the headstreams of the Tarim River. The following results were obtained. (1) The drought–flood index for the study area has been rising. The periodicities of the index were 4, 8, and 22 years with the periods of 4 and 8 years being significant. (2) The periodicities of annual runoff were 6, 17, and 22 years, with the 6-year period being the most significant. (3) The annual runoff of the Tarim River had significant negative correlation with the drought–flood index at multiple time-scales. The time sections of significant correlation were 2–10-year periods from the early 1970s to the late 1990s. (4) The drought–flood index had significant correlation with the NAO for periods of less than 10 years, which was negative mainly for the whole year and summer, and positive in winter. The aim of this study is to provide scientific guidance for achieving the reasonable allocation and regulation of water resources in the Tarim River Basin.

Key words | cross-wavelet, drought–flood index, headstreams of the Tarim River, multi-scale correlation, runoff process

Hongbo Ling
State Key Laboratory of Desert and Oasis Ecology,
Xinjiang Institute of Ecology and Geography,
Chinese Academy of Sciences,
Urumqi 830011,
China

Xiaoya Deng (corresponding author)
Aihua Long
State Key Laboratory of Simulation and Regulation of Water Cycle in River Basin,
Institute of Water Resources and Hydropower Research, Engineering and Technology Research Center for Water Resources and Hydro-ecology of the Ministry of Water Resources,
Beijing 100038,
China
E-mail: *84895430@qq.com*

Haifeng Gao
Chinese Academy of Sciences,
Institute of Tibetan Plateau Research,
Beijing 100101,
China

INTRODUCTION

According to the Fourth Intergovernmental Panel on Climate Change Report (2007), the global temperature has risen by 0.74 °C in the past 100 years (1906–2005), leading to accelerated global water circulation, an increase in precipitation, and the risk of more frequent flooding worldwide (Hu & Feng 2001; Zhang *et al.* 2008, 2015; Wang *et al.* 2013). One of the most significant potential consequences of changes in climate may be the alteration in regional hydrological cycles (Labat *et al.* 2004). The frequency of extreme events such as droughts and floods has been on the rise globally. As reported in the scientific literature, the changing patterns of drought–flood became a hot topic of research during 2001–2013 (Hu & Feng 2001; Gemmer *et al.* 2008; Zhang *et al.* 2008, 2010; Unami *et al.* 2010). Drought–flood variations are the result of several factors, with surface runoff and water resources being the main two factors. Considerable research has been carried out on the characteristics of drought–flood variation (Hu & Feng 2001; Gemmer *et al.* 2008; Zhang *et al.* 2008, 2010; Unami *et al.* 2010). The formation of surface runoff is closely related to climate factors (e.g., precipitation, temperature, and evaporation) and atmospheric circulation (Samaniego & Bardossy 2006; Brabets & Walvoord 2009; Karambiri *et al.* 2011). The response of runoff change to climate factors particularly results from the fluctuation in precipitation and temperature in arid and semi-arid regions (Gan 2000; Roger *et al.* 2006; Kamruzzaman *et al.* 2013; Dong *et al.* 2014). Therefore, discussing the effect of local climate change on runoff with a background of global change is important for sustainable social and economic development in a basin.

doi: 10.2166/nh.2016.166

The Tarim River Basin is the largest inland river basin in China, and is characterized by abundant natural resources and a fragile environment (Xu *et al.* 2011). As a typical pure-dissipation inland river in the northwestern arid areas of China, the main stream of the Tarim River has no groundwater abstraction, and the runoff supply depends on precipitation and glacial meltwater in the headstream mountain areas. Previous research (Chen & Xu 2005; Chen *et al.* 2006; Xu *et al.* 2006, 2011, 2013; Yang *et al.* 2011) has demonstrated that there has been a substantial increase in precipitation in Xinjiang, and flooding has been a serious problem in the Tarim River Basin. Previous studies (Chen & Xu 2005; Xu *et al.* 2010a, 2010b, 2011) have mainly focused on runoff and climate change in the Tarim River Basin, which indicated rising trends in runoff, precipitation, and air temperature. The variations of the regional and global climate are related to changes in the North Atlantic Oscillation (NAO), and these changes have had a profound effect on regional and global distributions of surface temperature and precipitation (Hurrell & Loon 1997; Shorthouse & Arnell 1999; Ye *et al.* 2004; Fu & Zeng 2005). The Tarim River Basin, located in the hinterland of Eurasia, is a closed watershed. It is important to study the trends in local climate records in the Tarim River Basin and recognize the presence of strong regional patterns of change associated with phenomena like the NAO. Therefore, using precipitation and runoff data for the headstream mountain areas in the past 50 years, this paper analyzes the periodic significance of runoff and the drought–flood index through wavelet analysis, and investigates the correlation between the drought–flood index and the NAO index at multiple time-scales employing a cross-wavelet spectrum. It is hoped that these results can serve as a reference for the reasonable allocation and regulation of water resources in the Tarim River Basin.

DATA AND METHODS

Data resources

Measurements of annual runoff (provided by the Administration of the Tarim River Basin) at five hydrological stations (Xiehela, Shaliguilanke, Wuluwati, Tongguziluoke, and Kaqun) in the headstream mountainous areas of the Tarim River from 1957 to 2008 were collected. The five stations are assumed to measure 'natural' runoff with negligible human disturbance. Precipitation data were recorded monthly at nine weather stations in the mountain areas (Xiehela, Shaliguilanke, Wuluwati, Heishan, Tongguziluoke, Aheqi, Turgat, Tashikurgan, and Kaqun) from 1957 to 2007, and these data have the characteristics of integrity and homogeneity according to a Standard Normal Homogeneity Test (Alexandersson 1986). An index of the NAO reveals its variability since 1846 (Hurrell 1995). The time series of NAO indexes used in this research are determined from the difference in monthly sea-level pressure between Gibraltar (36.1 °N, 5.4 °W) and Reykjavik (64.1 °N, 22.5 °W) from 1957 to 2007, reconstructed by the Climatic Research Unit at the University of East Anglia (UEA/CRU).

Study area

The Tarim River Basin is located in the Eurasian heartland, in southern Xinjiang, China, and passes through the Taklimakan desert. The river basin covers 28 counties and cities, 46 regiments in five prefectures of southern Xinjiang, with a total population of 8.257×10^6. It has nine water systems and 144 rivers in total, including the Aksu, Kashgar, Yarkand, Hotan, Kaidu, Kongqi, Dina, Weigan, Kuche, Keriya, and Qarqan rivers (Figure 1). The total area of the basin is 1.02×10^6 km^2, of which mountains account for 47%, plains for 20%, and desert for 33%. The long-term average 'natural' runoff is 398.3×10^8 m^3, and the total water resource is 428.4×10^8 m^3 for the whole Tarim River Basin. The average annual temperature is 10.6 °C to 11.5 °C, and the average annual precipitation was 116.8 mm during the late 1990s. The river basin belongs to the continental arid desert climate zone.

The length of the main stream of the Tarim River is 1,321 km, and the river basin has no runoff yield. The main stream has historically received water from the nine water systems of the Tarim River. Due to human activities and climate change, the Qarqan River, Keriya River, and Dina River separated from the main stream before the 1940s, and the Kashgar River, Kaidu River, Kongqi River, and Weigan River separated from the main stream after the 1940s. There are now only three headstreams – the Hotan River, Yarkand River, and Aksu River – flowing

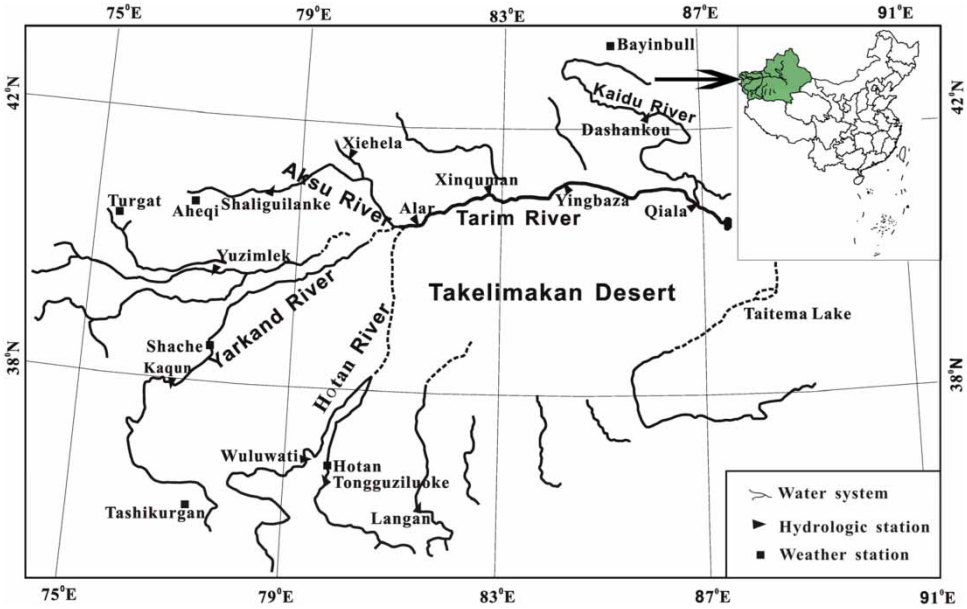

Figure 1 | Map of the Tarim River watershed.

into the main stream by Alar, accounting for 23.2%, 3.6%, and 73.2% of the total water volume, respectively.

Methods

In the study, the Z index was employed to divide the drought and flood grades of precipitation in the three headstreams of the Tarim River. Wavelet analysis was chose to explore the periods of drought–flood index and runoff, and the multi-time-scale correlations for drought–flood index to runoff and NAO.

Z index of precipitation

Four methods have been used to determine the drought–flood index in China: the anomaly percentage method, the Standardized Precipitation Index (SPI), the Z index method, and the humidity index method (Wu *et al.* 2001, 2011; Wang & Zhai 2003; Xue *et al.* 2015). Compared with the Z index method, the anomaly percentage method responds to drought and flood slowly and less sensitively, while the humidity index method responds quickly and is overly sensitive. The Z index can provide results similar to the SPI, but calculation of the Z index is relatively easy compared to the SPI (Wu *et al.* 2001). In addition, the coefficient of skew (c_s) is used in calculating the Z index, which means that Z relates to not only precipitation but also the regional precipitation distribution. When the coefficient of skew is larger, the analysis results of the Z index and its ability to reflect the degree of drought and flood improve (Zhang *et al.* 1998).

The China Z index has been used since 1995 by the National Climate Center of China as an operational real-time drought and flood monitoring tool (Wu *et al.* 2001; Zou *et al.* 2005). This paper analyzes the drought and flood conditions in the headstreams using the Z index method (Ju *et al.* 1998).

The time sequence of the precipitation is assumed to obey a Pearson III distribution (Wu *et al.* 2001; Zou *et al.* 2005). The probability density function is

$$f(x) = \frac{\beta_a}{\Gamma_{(a)}}(x - a_0)^{a-1}e^{-\beta(x-a_0)},\ (x > a_0) \tag{1}$$

where x is the random variable of interest and (a, a_0, β) represent the shape, location, and scale parameters, and $\Gamma_{(a)}$ is the gamma function. The mathematic expectation of the probability density function is

$$m = \frac{a}{\beta} + a_0 \tag{2}$$

and

$$a_0 = m\left(1 - \frac{2c_v}{c_s}\right) \tag{3}$$

$$a = \frac{4}{c_s^2} \tag{4}$$

$$\beta = \frac{2}{\sigma c_s} \tag{5}$$

where c_s is the coefficient of skew and c_v is the coefficient of variation. Both are attained from the precipitation sequence

$$c_s = \frac{\sum_{i=1}^{n}(x_i - \bar{x})^3}{m\sigma^3} \tag{6}$$

$$c_v = \frac{\sigma}{\bar{x}} \tag{7}$$

where σ is the standard variance of the precipitation sequence, $\bar{x}$ is the mean value of the precipitation sequence. The precipitation X is normalized by

$$x = \frac{a}{\beta}\left[1 - \frac{1}{9a} + z\left(\frac{1}{9a}\right)^{1/2}\right]^3 + a_0 \tag{8}$$

The probability density function is transformed from a Pearson III distribution to a standard normal distribution by taking Z as the variable:

$$z_i = \frac{6}{c_s}\left(\frac{c_s}{2}\varphi_i + 1\right)^{1/3} - \frac{6}{c_s} + \frac{c_s}{6} \tag{9}$$

where φ_i is the standard variable and is expressed as

$$\varphi_i = \frac{x_i - \bar{x}}{\sigma} \tag{10}$$

z_i is calculated using Equation (9). The regional drought–flood index is then obtained by

$$z = \frac{1}{n}\sum_{i=1}^{n} z_i \tag{11}$$

where z_i is the Z index of each station in the study area, and n is the total number of stations in the study area.

According to the normal distribution curve of variable Z (Zhang *et al.* 1998), seven grades of the Z index have been established for the drought–flood index as shown in Table 1.

Wavelet analysis

Wavelet analysis is becoming a common tool for analyzing localized variations of power within a time series, which has been increasingly used in hydrology (Torrence & Compo 1998). Wavelet analysis has recently been widely used in determining the periodicities of precipitation and runoff time series (Farge 1992; Stuart 2007; Li *et al.* 2009, 2013; Liu *et al.* 2009). Not only does it detect significant periodic variations of drought–flood index and runoff at different time-scales, but it analyzes the phase changes at different time-scales in our study. In wavelet analysis, the Morlet wavelet represents a wave modulated by a Gaussian function. The continuous wavelet transform coefficient is calculated by using a discrete signal with a Morlet wavelet. The wavelet variance is acquired based on the integral equation of the wavelet transform coefficient. The peak values of wavelet variance correspond to the significant periods of different time-scales. The periodic significance of wavelet variance is determined by a chi-square test (Torrence & Compo 1998). The edge errors usually occur at the beginning and end of a time series with finite length, because the wavelet is not completely localized in time (Torrence & Compo 1998; Zhang *et al.* 2008). To avoid these effects, the time series of the drought–flood index and runoff were symmetrically extended before wavelet transformation. Therefore, the

Table 1 | The grades of drought–flood index

Grade	Drought–flood index	Drought and flood type
1	$Z > 1.6485$	Extreme flood
2	$1.0364 < Z \leq 1.6485$	Serious flood
3	$0.5244 < Z \leq 1.0364$	Light flood
4	$-0.5244 < Z \leq 0.5244$	Normal
5	$-1.0364 < Z \leq -0.5244$	Light drought
6	$-1.6485 < Z \leq -1.0364$	Serious drought
7	$Z < -1.6485$	Extreme drought

1-year period was eliminated and the time series anomaly was used in the wavelet analysis (Torrence & Compo 1998; Zhang *et al.* 2008).

The cross-wavelet spectrum can describe in detail the correlations for the drought–flood index to runoff and NAO at different time-scales. A larger coefficient indicates better correlation. The significance of the wavelet spectrum is tested according to the red-noise standard spectrum (Torrence & Compo 1998). A ratio of wavelet spectrum to red-noise standard spectrum exceeding 1 indicates significant correlation (Torrence & Compo 1998).

RESULTS AND DISCUSSION

Classification of the drought–flood index

The *Z* index (i.e., the drought–flood index) was calculated by using the annual precipitation summed for the 16 monthly data at nine weather stations for 1957–2007 in the study area (Figure 2). Figure 2 shows that the drought–flood index has been rising in the headstreams of Tarim River Basin. For the drought and flood variations, 1957–1960 were normal years (i.e., there was no drought or flood) of drought and flood. During the period 1961–1969, there were two light flood years (1964 and 1966) and two serious drought years (1961 and 1969), and other years were normal. The variance of the drought–flood index increased and the climate was dominated by the drought conditions in the 1970s. Serious drought years transformed into light flood years in 1970–1972, the extreme drought years were 1973, 1975, and 1978, the light drought and serious drought years were 1977 and 1979, and other years were normal. In the 1980s, there were two light drought years (1980 and 1983), one serious drought year (1984), one extreme drought year (1985), two light flood years (1981 and 1988), and two serious flood years (1982 and 1987). Furthermore, there have been two serious drought years (1994 and 2000), two extreme flood years (1996 and 2005), four serious flood years (1993, 2001, 2002, and 2003), and four light flood years (1991, 1992, 1998, and 2004) since the 1990s.

Periodicity of the drought–flood index

Figure 3 presents a wavelet analysis of the drought–flood index for the headstream mountain areas of the Tarim River. In Figure 3(a), the drought–flood index represents the interdecadal change with a period of 22 years, which is also verified in Figure 3(b). In the 22-year period, the index abruptly changed from drought to flood in 1988 (Figure 3(b)). Additionally, the curve for the 22-year period was not closed in the positive-phase isogram for 2007, indicating that the drought–flood index would continue to denote a flood period in the coming years. The interannual change in the index was the most significant in the period range of 3–8 years, with the peak values of wavelet variance corresponding to 4-year and 8-year periods at a confidence level of 0.05 in the chi-square test. Positive and negative

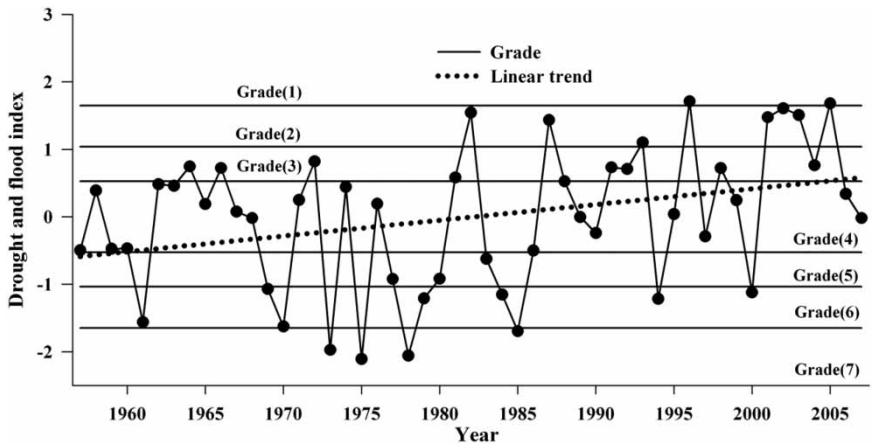

Figure 2 | Classification of drought–flood index in the headstreams of the Tarim River.

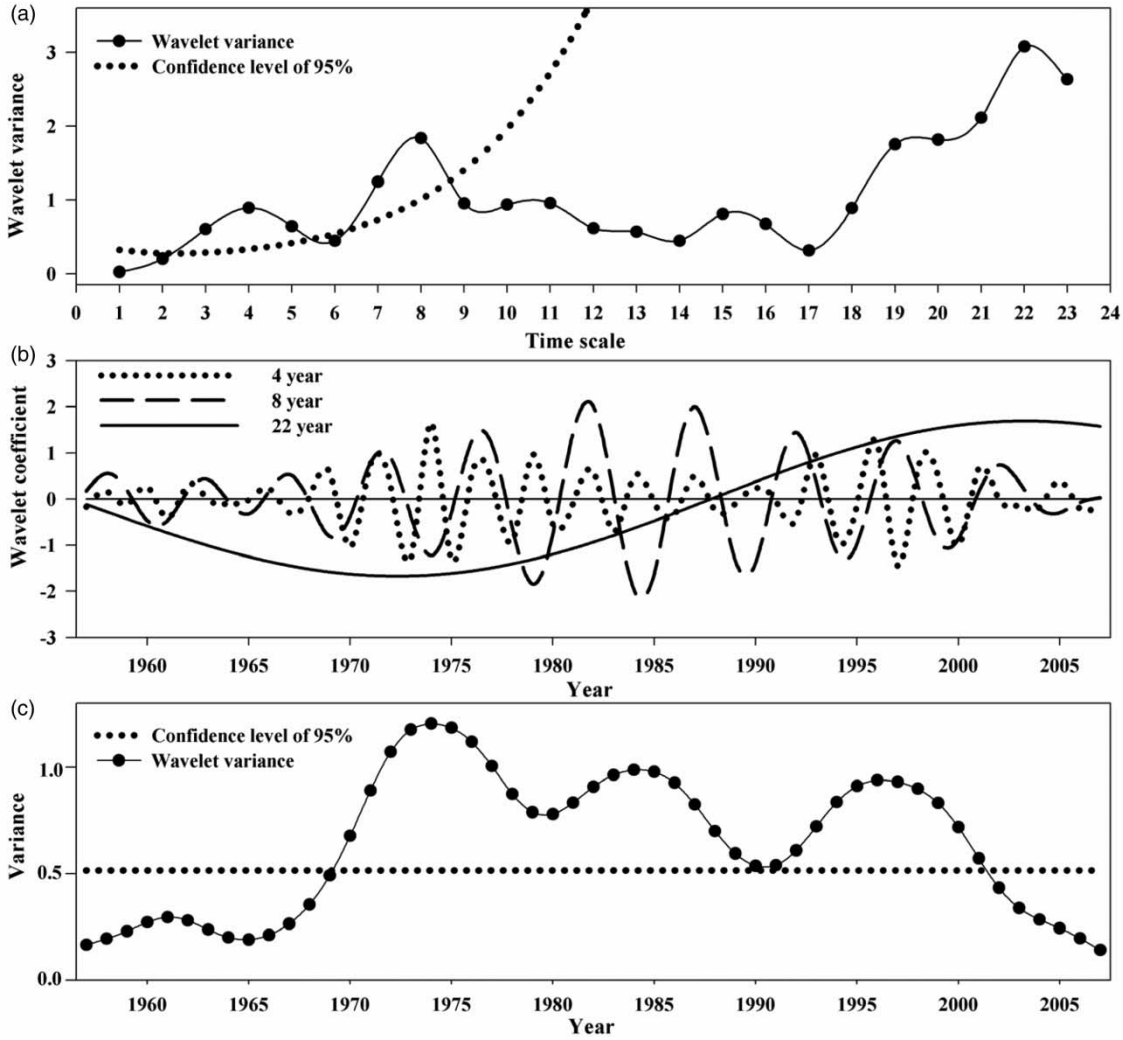

Figure 3 | Wavelet variances (a), wavelet coefficients (b), and significant time sections (c) of drought–flood indexes in the headstream mountain areas of the Tarim River. In (b), the positive wavelet coefficient indicates the positive phase (flood period), the negative wavelet coefficient indicates the negative phase (drought period), and zero value represents the abrupt change year of drought and flood.

phases represent periodic alternative variations with high frequency. Therefore, based on the wavelet coefficients of drought and flood indexes in the three primary periods (i.e., 4-year, 8-year, and 22-year) of the recent 50-year study period, the prediction equations were attained by nonlinear fitting to analyze the change characteristics in the future. Table 2 shows the wavelet coefficients of drought and flood indexes fitted significantly at a test level of 0.01, and it indicated that the prediction results of the fitting equations were reliable. Future values of drought and flood indexes in the significant periods can thus be calculated for the Tarim River. In addition, there was significant interannual change during the period 1970–2001 in the period of 3–8 years (Figure 3(c)).

Generally, regional climate change correlates closely with large-scale air circulation (João *et al.* 1998; Jaagus 2006; Fleming *et al.* 2016). There is a significant periodicity of approximately 3–8 years in the drought–flood index for the headstream mountain areas of the Tarim River, consistent with the periodicity of the El Niño/La Niña-Southern Oscillation (Trenberth *et al.* 2007).

Table 2 | Fitting equation of the period of the drought–flood index

Period of drought flood index (year)	Fitting equation	R^2	F	P
4	$Y = 0.5283\sin(2.2642x - 6.28) - 0.0145$	0.35	8.26	0.0002
8	$Y = 0.9876\sin(1.2752x + 6.28) - 0.0227$	0.59	22.26	<0.0001
22	$Y = 1.6871\sin(0.1003x + 1.708) + 0.004$	0.999	187697.44	<0.0001

'Y' is the period of the drought flood index, 'x' is the year series.

Periodicity of the annual runoff

Previous studies (Jiang *et al.* 2007; Xu *et al.* 2010a) have analyzed the runoff of the Tarim River by using the method of wavelet analysis; however, the significance of the runoff period had not been tested. In the wavelet analysis, there was apparently noise in the wavelet transformation resulting from random fluctuations in the original data. The raw data loss is more serious as the number of wavelet decompositions increases, and the confidence level for the period at longer time-scales is low. Therefore, we used a chi-square test for the significance of the period of annual runoff in the study area. In addition, wavelet analysis is time-dependent and is only meaningful within certain time ranges (i.e., the significant ranges) (Jiang 2008). Therefore, for the runoff of the Tarim River, the significant time range in the significant period has also been tested (Figure 4).

Figure 4(a) reveals that the main periodicities in the annual runoff of the three headstreams were 6, 17, and 22 years and that the main periods were significant at a confidence level of 95% for a 2–6-year period, but not significant for periods longer than 6 years. According to Figure 4(b), an alternative high-frequency oscillation was apparent in the annual runoff for the 6-year period. The abrupt change points of the 17-year period were in 1969, 1983, 1995, and 2008, and the phases had four abrupt changes (positive–negative–positive–negative). In addition, the annual runoff of the Tarim River abruptly changed in 1987 in terms of the 22-year period. According to the wavelet coefficients of runoffs in the three significant periods, the fitting equations were acquired to predict the future runoff change (Figure 4(c) and Table 3). Figure 4(c) shows that there were significant shorter periods in 1957–1967, 1970–1981, and 1988–1997 for 2–6-year periods at a confidence level of 95%.

Correlation analysis of drought–flood index and annual runoff

Figure 5 presents the multi-time-scale correlation between annual runoff and the drought–flood index for the headstream mountain areas of the Tarim River. In Figure 5, the drought–flood index was negatively correlated with the annual runoff at different time-scales in the past 50 years. However, this seems not to correspond to reality. A reason for this is that precipitation over the Tarim River headstreams is generally snow, which takes a long time to melt; the meltwater first flows into ground water and then overflows into runoff, resulting in a runoff lag to precipitation in time. In addition, the runoff supply from the headstreams mainly depends on glacier and snow meltwater, and therefore runoff is more closely correlated with temperature than with precipitation (Xu *et al.* 2011). When precipitation increases in a certain period of time, the temperature is thus low, and it will directly lead to a decrease of glacier and snow meltwater, and this decrease drives the runoff (and vice versa). As there is a positive correlation between temperature and runoff and a negative correlation between temperature and precipitation, the relationship between annual runoff and precipitation appears to be a negative correlation.

In the cross-wavelet spectrum, there was a positive correlation for periods over 20 years, but no significant correlation for the whole time series. The reason is that the original information loss becomes serious as the number of wavelet decompositions increases. The section of significant correlation encompasses the 2–10-year period from the early 1970s to the late 1990s. Specifically, the correlation is significantly negative in the 1970s for the 2–5-year period, the mid-1970s for the 7–8-year period, from the mid-1970s to the mid-1990s for the 9-year period, and in the early and mid-1990s for the 3–8-year period, and significantly positive in the early 1970s for the 8–9-year period, and the late 1970s and the early 1980s for the 7–8-year period.

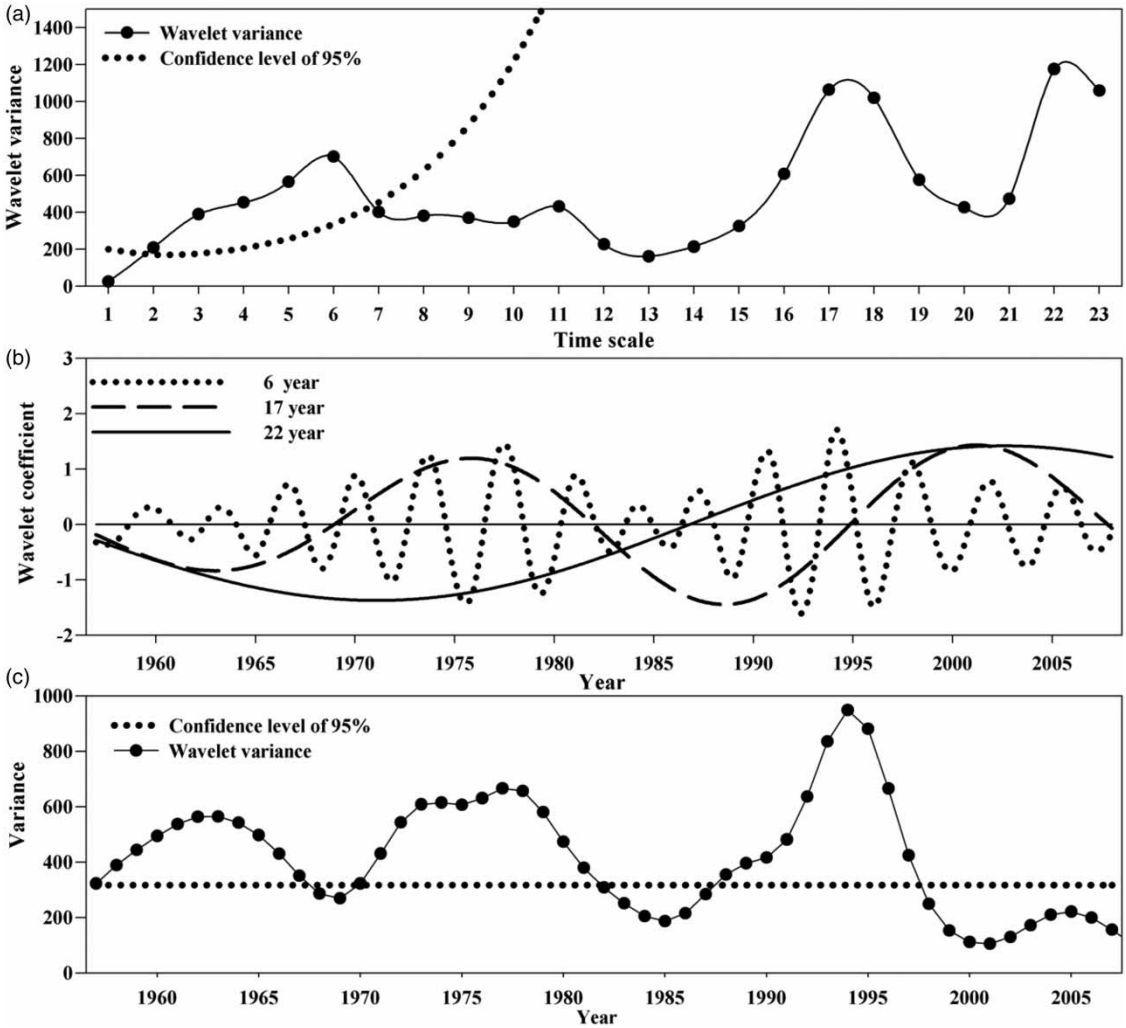

Figure 4 | Variances (a), wavelet coefficients (b), and significant time sections (c) of the annual runoff in the headstream mountain areas of the Tarim River.

Table 3 | Fitting equation of period of runoff in the headstreams of the Tarim River

Period of runoff (year)	Fitting equation	R^2	F	P
6	$Y = 0.693 \sin(1.771x - 6.28) + 0.0033$	0.47	14.03	<0.0001
17	$Y = 1.0186 \sin(0.2014x - 6.28) + 0.0086$	0.72	40.69	<0.0001
22	$Y = 1.3981 \sin(0.0987x + 5.0544) + 0.0146$	0.999	180262.00	<0.0001

'Y' is period of drought flood index, 'x' is year series.

Correlation between the drought–flood index and NAO index

Table 4 shows the relationship between the NAO index and the drought–flood index in Pearson and nonparametric tests. The drought–flood index and NAO index had insignificant negative correlation for the whole year, significant negative correlation in summer, and an extremely positive correlation at a test level of 0.01 in winter. The cross-wavelet spectrum was used for further discussion about the correlation between the drought–flood index and NAO index at multiple time-scales, as presented in Figure 6.

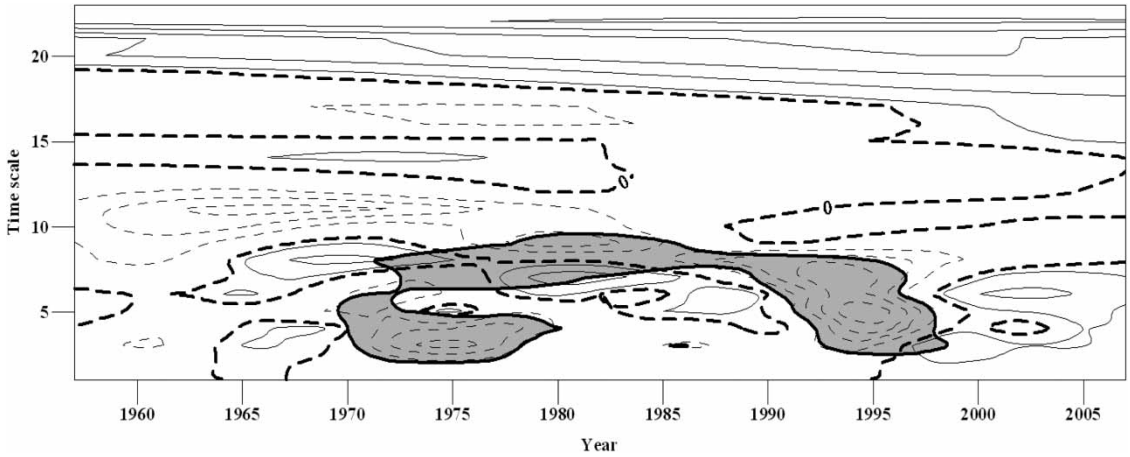

Figure 5 | Cross-wavelet analysis of annual runoff and drought–flood index in the headstream mountain areas of the Tarim River. The gray area indicates the significant correlation between annual runoff and drought–flood index at a confidence level of 95%, the solid line and dotted line, respectively, represent the positive correlation and negative correlation, and a bold dotted line indicates a transformation point of positive and negative phases.

Table 4 | Correlation between NAOI and drought–flood index in the headstreams of the Tarim River Basin

Item	Pearson test			Kendall's tau_b		
Correlation test	Annual	Winter	Summer	Annual	Winter	Summer
	−0.067	0.410**	−0.311*	−0.049	0.271**	−0.240*

'**' is significant at the test level of 0.01.
'*' is significant at the test level of 0.05.

Figure 6(a) reflects the multi-time-scale variation in the correlation between the drought–flood index and NAO index for the whole year, winter and summer. In the annual cross-wavelet spectrum, the correlation between the drought–flood index and NAO index was mainly negative, although it was significantly positive for periods longer than 21 years, and negative for the 15–21-year period. There was a positive correlation in the sections of significance in the 1970s in the 2–5-year period, and negative correlation from the mid-1990s to 2004. Furthermore, the correlation between the drought–flood index and NAO index was negative in 1985 to 1987 for the 4–5-year period, significantly negative in 1979 to 1986 for the 6–7-year period and from the late 1980s to the late 1990s, and negative for the 8–9-year period from the late 1970s to the late 1980s. The results demonstrate that the NAO index has affected the drought–flood index remarkably since the 1970s.

Figure 6(b) shows that there was a significant positive correlation between the NAO index and drought–flood index with the periods of 21–23 years, including the significant negative correlations of the 3–9-year period after 1985 in the winter. In Figure 6(c), there was a significant negative correlation between the NAO index and drought–flood index with the periods of 2–10 years in the summer. On the basis of this analysis, there is clearly a correlation between the drought–flood index and NAO index, especially for periods of less than 10 years. Therefore, we conclude that the NAO index affects drought and flood conditions by means of large-scale air circulation in the headstream mountain areas of the Tarim River. The Tarim River Basin is far from the sea, and vapor transport is thus restricted not only by vapor resources but also by the effect of terrain on air circulation. The southwest monsoon from the Indian Ocean is obstructed by the Himalaya Mountains and Tibet Plateau, which keep water from reaching Xinjiang. The southeast monsoon and tropical storms from the Pacific Ocean are meridional circulations and mainly affect the east of China because of the obstruction of the mountains

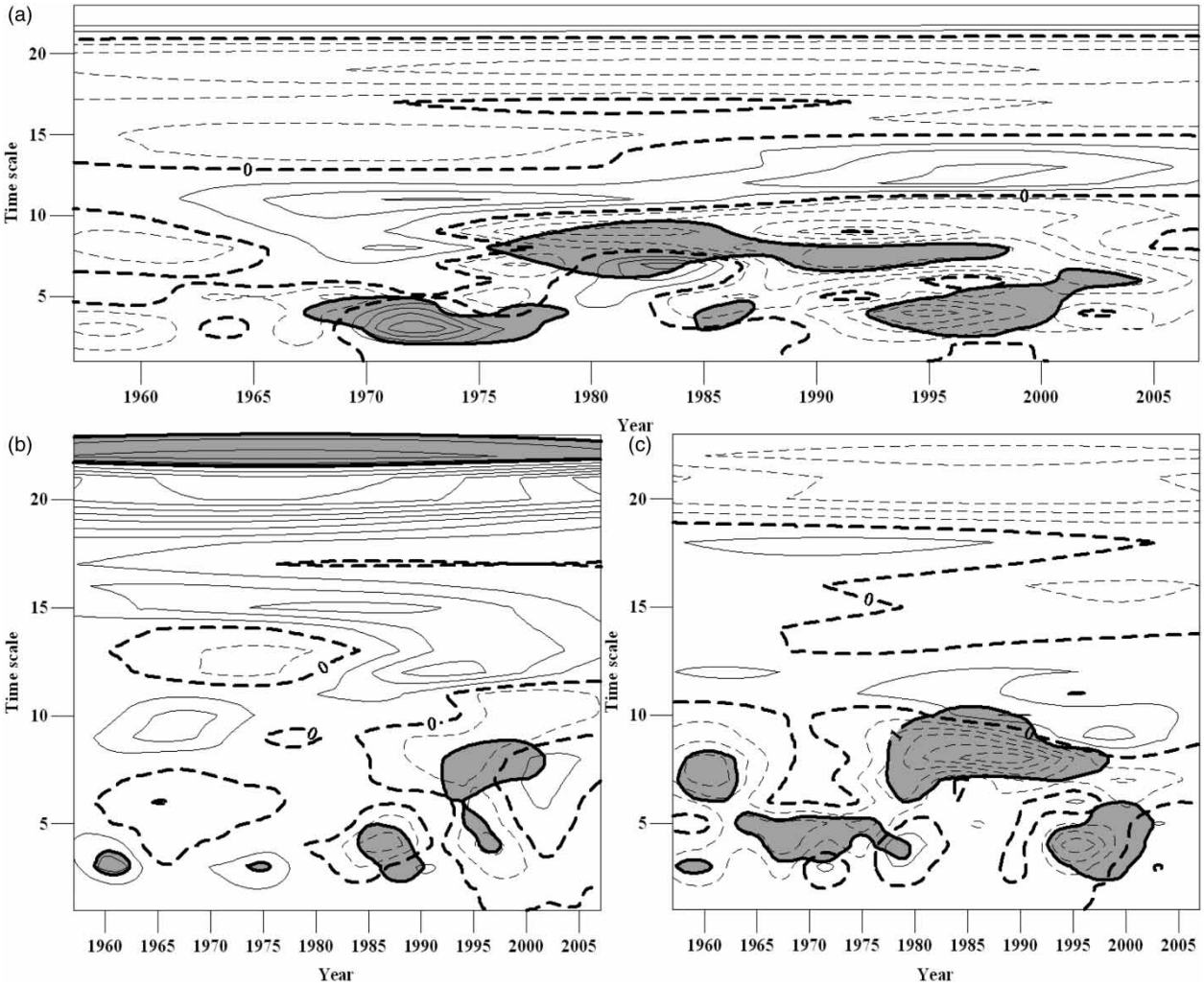

Figure 6 | Cross-wavelet analysis for the annual (a), winter (b), and summer (c) periods, between the drought–flood index and NAO index in the headstream mountain areas of the Tarim River.

and plateau. The Tarim River Basin is mid-latitude in the Northern Hemisphere and has prevailing westerlies. Therefore, the major resource of water vapor in the Tarim River Basin is westerly airflow from the Atlantic, followed by dry–cold airflow from the Arctic Ocean, and the water vapor quantity is 25–33% of west wind airflow (Zhou 1999).

CONCLUSIONS

It is found from the analysis of this paper that the drought–flood index has increased in the headstream mountain areas of the Tarim River in the past 50 years. Wavelet analysis showed that the drought–flood index had primary periodicity of 4, 8, and 22 years, with the periodicity of 4 and 8 years being significant. The period change during 1970–2001 was significant for the 3–8-year period.

The annual runoff of the headstreams in the Tarim River has had periodicity of 6, 17, and 22 years. Only the 6-year period is significant at a confidence level of 95%. A periodic zone of 2–6 years was significant during the periods 1957–1967, 1970–1981, and 1988–1997.

The correlation between the annual runoff and the drought–flood index at different time-scales was mainly negative. The significant time sections were the 2–10-year

periods from the early 1970s and the late 1990s, which demonstrate that the drought–flood index is significantly correlated with annual runoff.

The NAO has been in positive and high phase since the 1970s. The changes in drought–flood are linked to the behavior of the NAO. There was a significant correlation between the drought–flood index and the NAO index for periods of less than 10 years, which was negative mainly for the whole year and summer, and positive in winter. This indicates that the influences of the NAO on the drought–flood in the headstream mountain areas of the Tarim River are linked with the changes in upper air circulation. However, the effect mechanism of the NAO on annual runoff has not been explored and should be given further attention.

ACKNOWLEDGEMENTS

We thank four anonymous reviewers who provided helpful comments and suggestions. The corresponding author gratefully acknowledges the research group at the Ecological Complexity and Modeling Laboratory, University of California at Riverside. This work was funded by the National Natural Science Foundation of China (41471099, 51479209, and 41401050), the West Light Foundation of The Chinese Academy of Sciences (XBBS-2014-13) and the Science & Technology Cooperation Program of the Tarim River Basin (0202192014).

REFERENCES

Alexandersson, H. 1986 A homogeneity test applied to precipitation data. *J. Climatol.* **6**, 661–675.

Brabets, T. P. & Walvoord, M. A. 2009 Trends in streamflow in the Yukon River Basin from 1944 to 2005 and the influence of the Pacific Decadal Oscillation. *J. Hydrol.* **371**, 108–119.

Chen, Y. N. & Xu, Z. X. 2005 Plausible impact of global climate change on water resources in the Tarim River Basin. *Sci. China Ser. D.* **48**, 65–73.

Chen, Y. N., Takeuchi, K., Xu, C. C., Chen, Y. P. & Xu, Z. X. 2006 Regional climate change and its effects on river runoff in the Tarim Basin, China. *Hydrol. Process.* **20**, 2207–2216.

Dong, W., Cui, B. S., Liu, Z. H. & Zhang, K. J. 2014 Relative effects of human activities and climate change on the river runoff in an arid basin in northwest China. *Hydrol. Process.* **28**, 4854–4864.

Farge, M. 1992 Wavelet transforms and their applications to turbulence. *Annu. Rev. Fluid Mech.* **24**, 395–457.

Fleming, S. W., Hood, E., Dahlke, H. E. & O'Neel, S. 2016 Seasonal flows of international British Columbia-Alaska rivers: the nonlinear influence of ocean-atmosphere circulation patterns. *Adv. Water Resour.* **87**, 42–55.

Fu, C. B. & Zeng, Z. M. 2005 Correlations between North Atlantic Oscillation Index in winter and eastern China Flood/Drought Index in summer in the last 530 years. *Chinese Sci. Bull.* **50**, 2505–2516.

Gan, T. Y. 2000 Reducing vulnerability of water resources of Canadian Prairies to potential droughts and possible climate warming. *Water Resour. Manage.* **14**, 111–135.

Gemmer, M., Jiang, T., Su, B. D. & Kundzewicz, Z. W. 2008 Seasonal precipitation changes in the wet season and their influence on flood/drought hazards in the Yangtze River Basin, China. *Quatern. Int.* **186**, 12–21.

Hu, Q. & Feng, S. 2001 A southward migration of centennial-scale variations of drought/flood in eastern China and the western United States. *J. Climate* **14**, 1323–1328.

Hurrell, J. W. 1995 Decadal trends in the North Atlantic Oscillation: regional temperatures and precipitation. *Science* **269**, 676–679.

Hurrell, J. W. & Loon, H. V. 1997 Decadal variations in climate associated with the North Atlantic Oscillation. *Clim. Change.* **36**, 301–326.

IPCC Report 2007 *Climate Change 2007: Report of Working Group of the Intergovernmental Panel on Climate Change*. Cambridge University Press, Cambridge, pp. 16–72.

Jaagus, J. 2006 Climatic changes in Estonia during the second half of the 20th century in relationship with changes in large-scale atmospheric circulation. *Theor. Appl. Climatol.* **83**, 77–88.

Jiang, S. Z. 2008 Analysis on variety trend of runoff between Dari and Maqu in the headwater region of Yellow River in the past 50 years. *Geographical Res.* **27**, 221–228 (in Chinese).

Jiang, Y., Zhou, C. H. & Cheng, W. M. 2007 Streamflow trends and hydrological response to climatic change in Tarim headwater basin. *J. Geogr. Sci.* **17**, 51–61.

João, C., Qian, B. D. & Xu, H. 1998 Regional climate change in Portugal: precipitation variability associated with large-scale atmospheric circulation. *Int. J. Climatol.* **18**, 619–635.

Ju, X. S., Zou, X. K. & Zhang, Q. 1998 The method of the climatic drought-flood index and its analysis. *J. Natural Disaster* **7**, 51–57 (in Chinese).

Kamruzzaman, M., Beecham, S. & Metcalfe, A. V. 2013 Climatic influences on rainfall and runoff variability in the southeast region of the Murry-Darling Basin. *Int. J. Climatol.* **33**, 291–311.

Karambiri, H., Galiano, S. G. G., Giraldo, J. D., Yacouba, H., Ibrahim, B., Barbier, B. & Polcher, J. 2011 Assessing the impact of climate variability and climate change on runoff in West Africa: the case of Senegal and Nakambe River basins. *Atmos. Sci. Lett.* **12**, 109–115.

Labat, D., Ronchail, J., Callede, J., Guyot, J. L., De Oliveira, E. & Guimarães, W. 2004 Wavelet analysis of Amazon hydrological regime variability. *Geophys. Res. Lett.* **31**, L02501.

Li, H. J., Jiang, Z. H. & Yang, Q. 2009 Association of North Atlantic Oscillations with Aksu River runoff in China. *J. Geogr. Sci.* **19**, 12–24.

Li, L. F., Li, W. H. & Barros, A. P. 2013 Atmospheric moisture budget and its regulation of the summer precipitation variability over the Southeastern United States. *Clim. Dyn.* **41**, 613–631.

Liu, D. L., Liu, X. Z., Li, B. C., Zhao, S. W. & Li, X. G. 2009 Multiple time scale analysis of river runoff using wavelet transform for Dagujia River Basin, Yantai, China. *Chin. Geogr. Sci.* **19**, 158–167.

Roger, N. J., Francis, H. S. C., Walter, C. B. & Zhang, L. 2006 Estimating the sensitivity of mean annual runoff to climate change using select hydrological models. *Adv. Water Resour.* **29**, 1419–1429.

Samaniego, L. & Bardossy, A. 2006 Simulation of the impacts of land use/cover and climatic changes on the runoff characteristics at the mesoscale. *Ecol. Modell.* **196**, 45–61.

Shorthouse, C. & Arnell, N. 1999 The effects of climatic variability on spatial characteristics of European river flows. *Phys. Chem. Earth* **24**, 7–13.

Stuart, N. L. 2007 Assessment of rainfall-runoff models based upon wavelet analysis. *Hydrol. Process.* **21**, 586–607.

Torrence, C. & Compo, G. P. 1998 A practical guide to wavelet analysis. *B. Am. Meteorol. Soc.* **79**, 61–78.

Trenberth, K. E., Jones, P. D., Ambenje, P., Bojariu, R., Easterling, D., Klein, T. A., Parker, D., Rahimzadeh, F., Renwick, J. A., Rusticucci, M., Soden, B. & Zhai, P. 2007 *Observations: Surface and Atmospheric Climate Change*. Cambridge University Press, Cambridge, UK, pp. 235–336.

Unami, K., Abagale, F. K., Yangyuoru, M., Alam, A. M. B. & Kranjac, B. G. 2010 A stochastic differential equation model for assessing drought and flood risks. *Stoch. Environ. Res. Risk. Assess.* **24**, 725–733.

Wang, Z. W. & Zhai, P. M. 2003 Climate change in drought over northern China during 1950–2000. *Acta Geogr. Sin.* **58**, 61–68.

Wang, S. J., Zhang, X. L., Liu, Z. G. & Wang, D. M. 2013 Trend analysis of precipitation in the Jinsha River Basin in China. *J. Hydrometeorol.* **14**, 290–303.

Wu, H., Hayes, M. J., Weiss, A. & Hu, Q. 2001 An evaluation of the standardized precipitation index, the China-Z-index and the statistical Z-score. *Int. J. Climatol.* **21**, 745–758.

Wu, Z. Y., Lu, G. H., Wen, L. & Lin, C. A. 2011 Reconstructing and analyzing China's fifty-nine year (1951–2009) drought history using hydrological model simulation. *Hydrol. Earth Syst. Sci.* **15**, 2881–2894.

Xu, C. C., Chen, Y. N., Li, W. H. & Chen, Y. P. 2006 Climate change and hydrologic process response in the Tarim River Basin over the past 50 years. *Chinese Sci. Bull.* **51**, 125–136.

Xu, J. H., Li, W. H., Ji, M. H., Lu, F. & Dong, S. 2010a A comprehensive approach to characterization of the nonlinearity of runoff in the headwaters of the Tarim River, western China. *Hydrol. Process.* **24**, 136–146.

Xu, Z. X., Liu, Z. F., Fu, G. B. & Chen, Y. N. 2010b Trends of major hydroclimatic variables in the Tarim River basin during the past 50 years. *J. Arid Environ.* **74**, 256–267.

Xu, H. L., Zhou, B. & Song, Y. D. 2011 Impacts of climate change on headstream runoff in the Tarim River Basin. *Hydrol. Res.* **42**, 20–29.

Xu, C. C., Chen, Y. N., Chen, Y. P., Zhao, R. F. & Ding, H. 2013 Responses of surface runoff to climate and human activities in the arid region of Central Asia: a case study in the Tarim River Basin, China. *Environ. Manage.* **51**, 926–938.

Xue, F. C., Song, X. Y., Shen, D. D. & Wang, J. 2015 Evaluating agricultural drought hazard risk based on GIS-MCE. *Int. J. Adapt. Control.* **8**, 389–400.

Yang, Y. H., Chen, Y. N., Li, W. H., Yu, S. L. & Wang, M. Z. 2011 Climatic change of inland river basin in an arid area: a case study in northern Xinjiang, China. *Theor. Appl. Climatol.* **106**, 481–488.

Ye, H. C., Yang, D. Q., Zhang, T. J., Zhang, X. B., Ladochy, S. & Ellison, M. 2004 The impact of climatic conditions on seasonal river discharges in Siberia. *J. Hydrometeorol.* **5**, 286–295.

Zhang, G. J., Wang, B. L., Liu, D. X. & Cai, Z. L. 1998 Research on drought and flood indices the northwest China. *Plateau Meteorol.* **17**, 381–389 (in Chinese).

Zhang, Q., Chen, Y. D. & Chen, J. Q. 2008 Flood/drought variability in the Yangtze Delta and association with the climatic changes from the Guliya ice core: a wavelet approach. *Quatern. Int.* **189**, 163–172.

Zhang, Q., Yu, Z. G., Xu, C. Y. & Anh, V. 2010 Multifractal analysis of measure representation of flood/drought grade series in the Yangtze Delta, China, during the past millennium and their fractal model simulation. *Int. J. Climatol.* **30**, 450–457.

Zhang, X. L., Wang, S. J., Zhang, J. M., Wang, G. & Tang, X. Y. 2015 Temporal and spatial variability in precipitation trends in the Southeast Tibetan Plateau during 1961–2012. *Clim. Past (Discussions).* **11**, 447–487.

Zhou, Y. C. 1999 *Hydrology and Water Resources for the Rivers in Xinjiang*. Health Science and Technology, Xinjiang, Urumqi, pp. 14–15.

Zou, X. K., Zhai, P. M. & Zhang, Q. 2005 Variations in droughts over China: 1951–2003. *Geophysical Res. Lett.* **32**, L04707.

First received 4 August 2015; accepted in revised form 29 February 2016. Available online 31 March 2016